Iranian Journal of Geophysics, Vol 15 No 4, 2022, Page 115 – 126 (Research Article)
DOI: 10.30499/IJG.2021.296842.1347

A Seismic investigation of the upper crustal structure of the Iranian plateau

Mohsen Ahmadzadeh Irandoust[1], Keith Priestley[2] and Farhad Sobouti[3*]

[1] *PhD Student of Geophysics, Department of Earth Sciences, Institute for Advanced Studies in Basic Sciences (IASBS), Zanjan, Iran*
[2] *Professor of Geophysics, Bullard Laboratories, Department of Earth Sciences, University of Cambridge, Cambridge, UK*
[3] *Associate Professor of Geophysics, Department of Earth Sciences, Institute for Advanced Studies in Basic Sciences (IASBS), Zanjan, Iran*

(Received: 26 July 2021, Accepted: 25 November 2021)

Abstract

We obtained a three-dimensional (3D) shear wave velocity model of the upper crust of the Iranian Plateau, based on the inversion of fundamental mode Rayleigh wave group velocity. The surface wave group velocity measurements for the period range 5-25 s were extracted from two seismic data sets: ambient noise cross-correlations and regional earthquakes. The low shear wave velocity (V_s) anomalies of the upper crust correspond to regions of thick sediments. The surrounding basins of the Plateau, the South Caspian Basin (SCB) in the north and the Zagros Fold-Thrust Belt (ZFTB) and the Makran accretionary wedge in the south form the thickest sedimentary covers of the region exceeding 20 km. The thickest parts of inland basins such as the Jazmurian depression and the Dasht-e Kavir are ~10 km. The V_s structure of southern Zagros is almost homogeneous at all levels of the crust, but the low velocity anomaly beneath the southern Lorestan Arc separates the central Zagros from the northernmost Zagros. The volcanic belt of the Makran Subduction Zone forms another large/deep low velocity zone, where the observed low V_s possibly results from magma migration and heat transfer from the mantle wedge of the subduction zone. High velocity regions in the upper crust are observed in the Sanandaj-Sirjan Zone (SSZ), the Urmia-Dokhtar Magmatic Assemblage (UDMA), and in the south of the Lut Block.

Keywords: Iranian Plateau, upper crustal structure, sedimentary basin, Rayleigh wave, shear wave velocity

[*] Corresponding author: farhads@iasbs.ac.ir

1 Introduction

A continent-continent collision can thicken the crust, and the surface uplift accompanying the collision can create a plateau. The Arabia-Eurasia collision which initiated about ~25 Ma is similar to the Indo-Eurasian collision (initiated ~55 Ma) which created the Himalayas and Tibet (Hatzfeld and Molnar, 2010). Studies of the Zagros collision zone and the Iranian Plateau can provide clues to understanding the earlier stages of continental collision processes.

The Iranian Plateau (Fig. 1) accommodates ~22 mm/yr (e.g., Vernant et al., 2004a, 2004b; Khorrami et al., 2019) of the northward motion of the Arabian Plate relative to Eurasia. The deforming zone is bounded by the Zagros orogeny in the west and south, the Makran Subduction Zone in the southeast, the Afghan Block in the east, and the Alborz and Kopeh Dagh Mountains in the north. The Plateau consists of several aseismic rigid blocks that are trapped between the compressional belts. This tectonic structure results in various styles of deformation in different parts of the collision zone. Crustal shortening and thickening occur in the mountain ranges of Zagros, Talesh, Alborz, Binalud, and Kopeh Dagh, while NS strike-slip faulting system takes place in central and eastern Iran, and subduction occurs beneath the Makran. In the western part of the Iranian Plateau, the Zagros Mountains accommodate ~10 mm/yr of the convergence (e.g., Tatar et al., 2002) and the remaining part is taken up in the Alborz Mountains and the Apsheron subduction in the Caspian Sea (Priestley et al., 1994; Jackson et al., 2002). In the southeast, the Makran subduction accommodates about half of the northward motion of Arabia with the remainder accommodated in the mountain belts of the northeast part of the Plateau (e.g., Vernant et al., 2004a; 2004b).

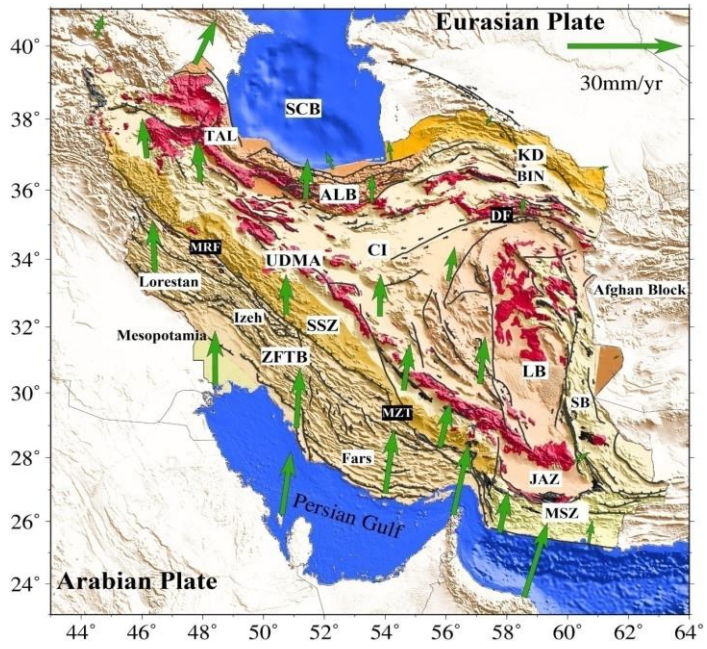

Fig 1. Geological map of Iran. The abbreviations are: Zagros Fold-Thrust Belt (ZFTB), the Sanandaj-Sirjan Zone (SSZ), the Urmia-Dokhtar Magmatic Assemblage (UDMA), Makran Subduction Zone (MSZ), the Jazmurian depression (JAZ), the Sistan Belt (SB), the Lut Block (LB), Kopeh Dagh (KD), the Binalud Mountains (BIN), Central Iran (CI), the South Caspian Basin (SCB), the Alborz Mountains (ALB), the Talesh Mountains (TAL), the Main Recent Fault (MRF) and the Main Zagros Thrust (MZT). Solid lines represent the active faults (Hessami et al., 2003). GPS velocity vectors are from Vernant et al. (2004b).

Iran is one of the most seismically active regions in the world and the relationship between seismicity, distribution of surface tectonics and faulting systems, and the deeper structures of the crust and uppermost mantle can provide fundamental insight into the continental deformation processes. The production of a comprehensive velocity model for the upper crust enables us to provide insight into these issues, as well as increase the understanding of the nature of the regional continental deformation.

The lithosphere of the Iranian Plateau has been previously investigated using different seismic tomography techniques (e.g., Maggi and Priestley, 2005; Shad Manaman et al., 2011; Priestley et al., 2012; Rahimi et al., 2014; Movaghari and Javan Doloei, 2020; Kaviani et al., 2020; Movaghari et al., 2021), but more detailed studies are required to constrain the geodynamical evolution of the region. To this end, we have assembled a data set of ambient noise and regional earthquakes to extract fundamental mode Rayleigh wave group velocity measurements to build a three-dimensional (3D) model of the upper crust. We inverted one-dimensional (1D) path-averaged group velocities in the period range 5-25 s to get two-dimensional (2D) maps of group velocity. Variations in the dominant trends of velocity provide clues to the geological deformation of the region. In the following sections, the data and method used in this study are introduced. We then present the group velocity tomograms and shear wave velocity models at different depths, and discuss their relationship with the geology of the region.

2 Data and Methodology

The data for this research come from a large number of permanent and temporary broadband seismic stations located over the whole of Iran and the surrounding region. We used data from the permanent stations of the broadband Iranian National Seismic Network (INSN) and the Iranian Seismological Center (IRSC). In addition, recordings from stations in the surrounding regions were obtained from the Incorporated Research Institution for Seismology (IRIS) Data Center. Data from the permanent seismographs were supplemented by seismograms from five temporary seismic networks operated by the Institute for Advanced Studies in Basic Sciences (IASBS) and the University of Cambridge, as well as the CIGSIP array (the China-Iran Geological and Geophysical Survey in the Iranian Plateau). To enlarge the dispersion data set, we merged our dispersion measurements with the dispersion measurements of Gilligan and Priestley (2018). Fig. 2 shows the locations of the stations used for both ambient noise and regional earthquake measurements.

To obtain fundamental mode Rayleigh wave group velocity dispersion curves constraining the upper crust, we used inter-station ambient noise cross-correlations and regional earthquake-station pairs. The combination of the two data sets provides a better lateral and depth coverage and will reveal more structural detail of the study area. We obtained group velocity dispersion curves using the multiple filter analysis (MFT) program (Herrmann, 2013). More than 10400 vertical component seismic recordings from regional earthquakes (at epicentral distances between 100 and 5000 km) with magnitude $\geqslant$ 4 were analyzed. The calculated group velocity dispersion curves from the earthquakes are mostly in the 15 to 25 s period range. In addition, some shorter period dispersion curves were measured from earthquakes, too. To compensate for the lack of shorter period measurements from the earthquakes, we added group velocity dispersions from ambient noise cross-correlations (mostly 5 to 25 s) recorded at the sites indicated in Fig. 2. Before ex-

tracting the ambient noise Green's functions, the raw seismic data were processed as outlined in Bensen et al. (2007). First, the vertical component time series were decimated to 1 Hz and the continuous time series were cut to day-long segments. The instrument response, mean and trend were removed and a band-pass filter of 0.01-0.5 Hz was applied on the time series. Then, a running absolute mean as a time-domain normalization was applied to reduce the effect of earthquakes on the cross-correlations and the time series were spectrally whitened. Finally, the processed time series for each station pair were cross-correlated. To increase the signal-to-noise ratio of the final cross-correlations, the station-pair cross-correlated time series were stacked.

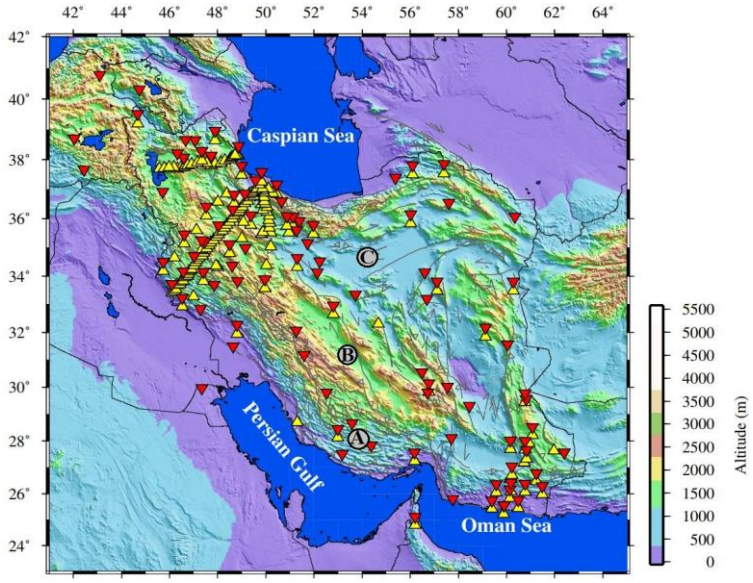

Fig 2. Distribution of the seismic stations used in this study. The red and the yellow symbols show the locations of the stations we used for the analysis of ambient noise cross-correlations and regional earthquakes, respectively. The inversion of Rayleigh wave group velocity for points A, B, and C are shown in Fig. 5.

In the next step, the dispersion data were tomographically inverted to obtain fundamental mode Rayleigh wave group velocity dispersion maps at ten periods between 5 and 25 s. First, a grid with a 1°×1° spacing covering the study region was constructed. Then, the inversion method of Debayle and Sambridge (2004) was employed to invert path-averaged surface wave dispersion measurements. This method is based on the continuous regionalization of Montagner (1986) in which physical properties of the model are considered as a priori information. The variation of Rayleigh wave velocity with propagation direction (Smith and Dahlen, 1973) involves one isotropic coefficient and two anisotropic coefficients associated with the 2θ terms. The Debayle and Sambridge (2004) inversion retrieves the three unknowns for each grid point of the two-dimensional (2D) model. We do not discuss the azimuthal anisotropy results for the upper crust but have included it in the inversion so as to not bias the isotropic results.

For a source-receiver path j, we have:

$$\frac{1}{Ud_j(T)} = \frac{1}{\Delta_j}\int_{E_j}^{S_i}\frac{ds_i}{U(T.\theta.\phi)} \qquad (1)$$

where $Ud_j(T)$ is the group wave-speed at period T measured along the path, θ and ϕ are the coordinates of the geographical points along the great circle, and Δ_j is the source-receiver distance. $U(T.\theta.\phi)$ is the local group wave speed at the geographical point. Using the great circle approx-

imation, the inverse problem can be written as a linear relationship between the data vector **d** containing the average group slowness 1/U(T.θ.ϕ) along each path and a parameter vector **m** containing the local group slowness 1/U(T.θ.ϕ) at each geographical point along the path. For a segmented jth path δs, we can write:;

$$\boldsymbol{d} = G\boldsymbol{m} \quad (2)$$

where the matrix G contains the partial derivatives $\delta s/\Delta_j$. A Gaussian a priori covariance function controls the horizontal degree of smoothing in the inverted model. By employing the formulation of Montagner (1986), the Debayle and Sambridge (2004) scheme incorporates sophisticated geometrical algorithms which dramatically increase computational efficiency of the inversion. Fig. 3 shows Rayleigh wave group velocity maps obtained for some of the periods.

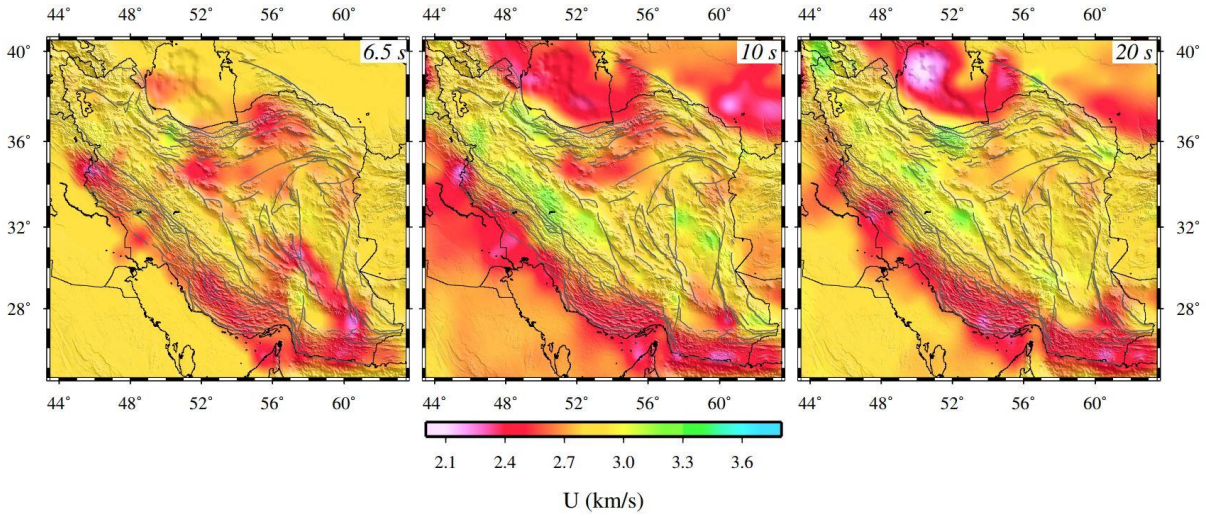

Fig 3. Results of fundamental mode Rayleigh wave group velocity tomography at different periods.

Checkerboard tests are among the common procedures to examine the resolution and retrieval strength of seismic wave tomography maps. Parameters like density and azimuthal gap of ray path distribution can affect the test result. Here we performed checkerboard tests using synthetic input models with 2° and 1° square-shaped alternating patterns of high and low velocities. The velocity perturbations of the synthetic input for different periods are ~+/- 0.35 km/s with respect to the mean velocity of the input data. Fig. 4 shows the raypath coverage of the measurements and the results of the checkerboard test at periods of 6.5, 10, and 20 s. The checkerboard tests indicate that both 2° and 1° checkers are mostly well resolved across the Plateau.

We next constructed pseudo-dispersion curves for each node point and inverted these curves for the shear wave velocity profiles using the linearized least-squares inversion algorithm of Herrmann (2013) with a finely parameterized starting structure (2 km-thick flat-lying). The wave speed of the crustal model used in starting the inversion is based on the uppermost mantle wave speed of AK135 (Kennett et al., 1995). Fig. 5 illustrates the steps taken for the inversion of Rayleigh wave group velocities at three geologically different regions: The Fars Arc, the SSZ, and the Dasht-e Kavir (see Fig. 2 for the locations).

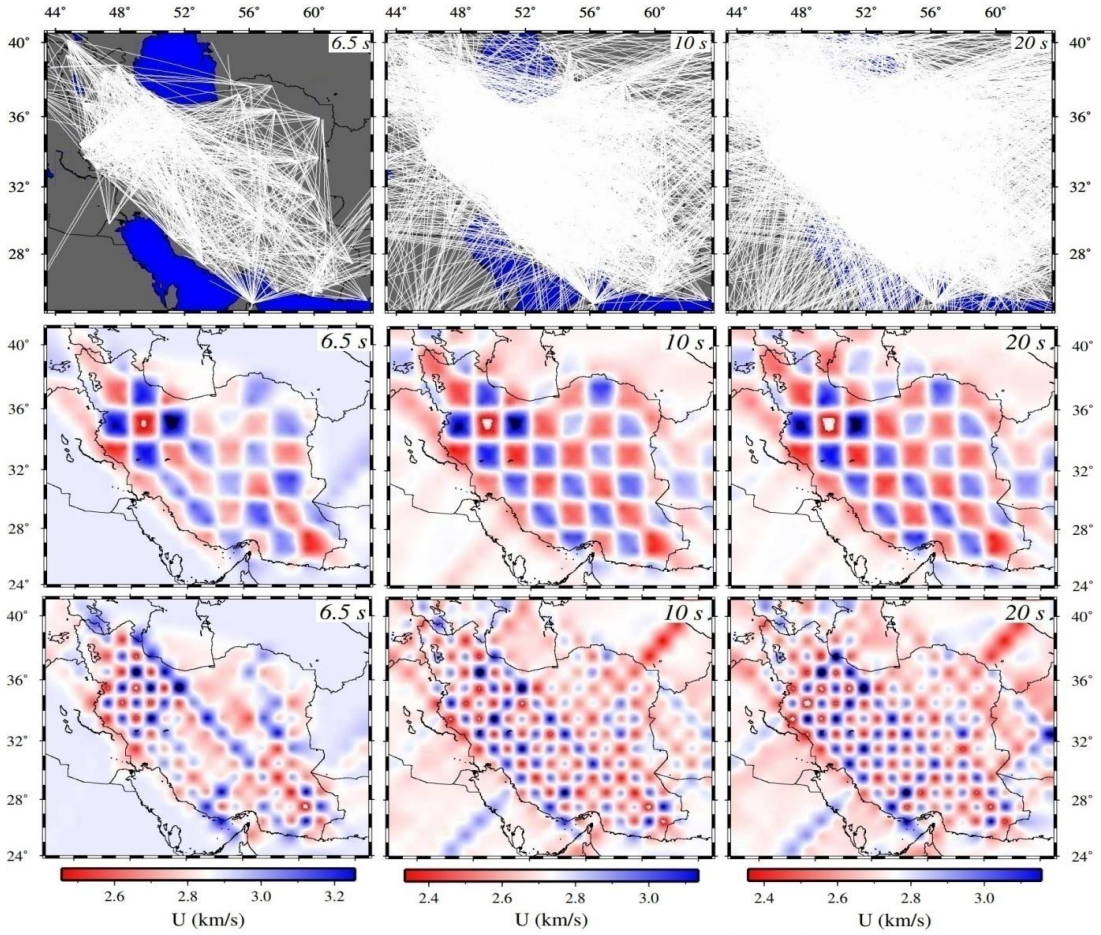

Fig 4. Raypath coverage and output models of the checkerboard test (2° and 1°) at periods 6.5, 10 and 20 s.

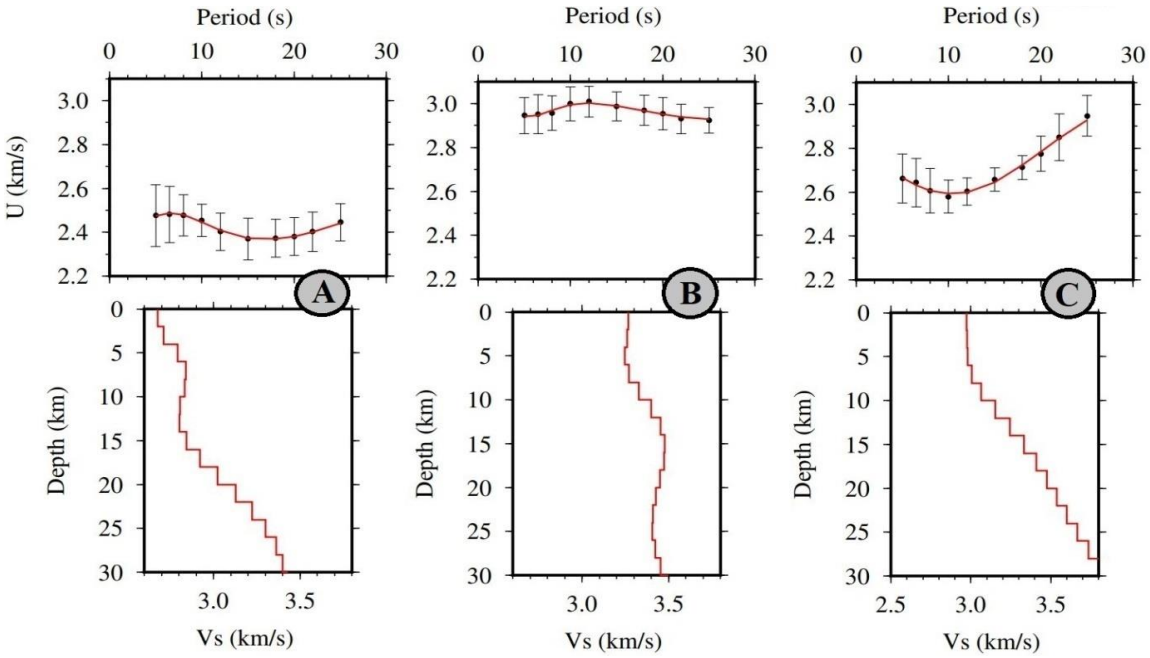

Fig 5. Examples of fundamental mode Rayleigh wave group velocity inversion to shear wave velocity model at points A, B, and C shown in Fig. 2. Upper panels: The observed dispersion curves (black dots with error bars) and the synthetic dispersion curves for the final velocity model (solid red line). Lower panels: The final V_s model (solid red line).

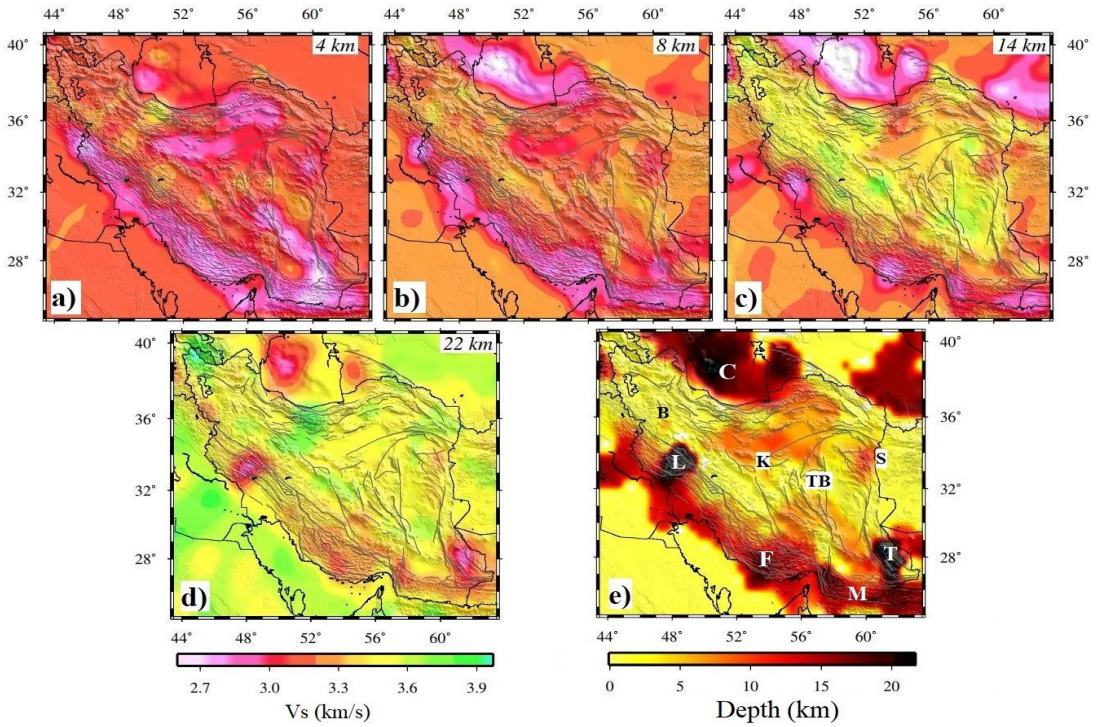

Fig 6. (a-d) Maps of shear wave velocity (V_s) at different depths. (e) Variations of the depth of shear wave velocity of 3.1 km/s which can represent regions of thick sediment or anomalously warm crust.

3 Results and Discussion

Fig. 3 shows the group velocity maps for periods 6.5, 10, and 20 s. The short period waves (< 25 s) are primarily sensitive to the upper crust. There is a strong correlation between the thick sedimentary basins of the upper crust and low short period group velocities (Laske et al., 2013). The South Caspian Basin (SCB), the Zagros Fold-Thrust Belt (ZFTB), the Makran accretionary wedge, and the Dasht-e-Kavir all show very low group velocities. The volcanic belt of the Makran Subduction Zone also has anomalously low velocities. The Sanandaj-Sirjan Zone (SSZ) and the Urmia-Dokhtar Magmatic Assemblage (UDMA) have higher velocities for the same period range. The lowest group velocities (< 2.2 km/s) are seen in the SCB, the boundary of the Lorestan Arc in western Zagros and Mesopotamian basin, and the Makran accretionary wedge. The SCB remains very low for all periods. The Taftan and Bazman volcanoes of the Makran Subduction Zone stand out as low-velocity regions compared to their surrounding areas.

Fig. 6 shows the maps of shear wave velocity (Vs) variations to a depth of 22 km in our model. Vs in the upper crust (< 20 km) is lowest (< 3.1 km/s) in regions of thick sediment in the Zagros Foreland Basin, the Makran accretionary wedge, the SCB, and to a lesser extent in the Dasht-e Kavir, the southern margin of the Dasht-e Lut, the Jazmurian basin, the northern end of the Sistan belt, and the lowland region connecting the eastern Alborz to the Kopeh Dagh Mountains. The lowest upper crustal V_s (< 2.7 km/s) occurs beneath the SCB, the Simply Folded Belt (SFB) of Zagros and the Makran Subduction Zone and its volcanic arc. In the uppermost crust (< 5 km) depth range, most of the Plateau shows velocities lower than 3.2 km/s. Higher V_s anomalies (3.2 to 3.4 km/s) in western Alborz, SSZ and UDMA, and the central Dasht-e Lut represent contrasts to their surroundings. In the deeper layers of the upper crust, in the depth range 10-20 km, the high velocity rocks (~3.7 km/s) which are the typical medium of the lower crust, are present in SSZ, UDMA, the Lut

Block, central Alborz, and eastern Binalud.

In the ZFTB, a thick sedimentary cover (maximum of ~12-16 km) has been reported (e.g., Alavi, 2007; Teknik and Ghods, 2017) overlying the crystalline basement. Our model for the Zagros orogeny generally shows a thick layer (5-15 km) of low V_s beneath the foreland basin and the ZFTB, decreasing in thickness beneath the High Zagros, and thinning out beneath SSZ and UDMA. The SFB shows low-velocity upper crust, but the Izeh Zone which exhibits a quite different crustal deformational morphology from the Lorestan and Fars arcs (Fig. 1), has a higher V_s upper crust. There are two deep low V_s anomalies (> 15 km-thick) located in the southern Lorestan Arc (labelled "L" in Fig. 6-e) which is adjacent to the Mesopotamia Basin and the Izeh Zone, and the central part of the Fars Arc (labelled F in Fig. 6-e). Our model confirms these two regions as the deepest sedimentary covers of the Zagros. Region "F" of the Fars shows low velocities as deep as ~18 km. The Lorestan low V_s anomaly goes even deeper to more than 20 km and extends under the SSZ. Recent studies by Maheri-Peyrov et al., (2020) and Movaghari and Javan Doloei, (2020), have reported a low-velocity anomaly for the upper crust of the Lorestan region based on local P wave velocity and Rayleigh wave phase velocity results, respectively. The large low velocity zone in the Lorestan comprising the whole upper and middle crust can be related to another mechanism besides a thick layer of sediment. Regarding the high seismicity pattern of this region (e.g., Karasözen et al., 2019), the low V_s crust can be interpreted as the combination of a thick layer of sediments on top of a crushed crystalline basement. The occurrence of high V_s rocks (3.7 km/s) in the upper crust of the SSZ can imply exhumation (e.g., François et al., 2014; Barber et al., 2018) as a result of the crustal-scale underthrusting of the Arabian Plate under central Iran (Paul et al., 2006, 2010; Mouthereau, 2011; Movaghari et al., 2021).

The Makran Subduction Zone has one of the widest and thickest accretionary wedges in the world (e.g., Kopp et al., 2000). The coastal Makran has a wide-band (> 100 km) of low velocity anomaly < 3.1 km/s (with label "M" in Fig. 6-e) exceeding a thickness of 15 km. Our estimation for the thickness of the sedimentary cover on the coastal Makran is ~12 km at ~62°E deepening to ~20 km to the east and west. The sedimentary cover overlying the Oman Sea oceanic plate has been measured to 7 km (White and Louden, 1983; Kopp et al., 2000). In the coastal Makran, Movaghari et al. (2014) and Penney et al. (2017) found the sedimentary section to be 22 and 26 km thick, respectively. Motaghi et al. (2020) suggested that the base of the accretionary wedge is gently deepening from 9 to 15 km, and Heberland Haberland et al., (2020) estimated a maximum thickness of the accretionary wedge to be 35 km.

The velocity models of this study (Figs. 3 and 6) indicate that the upper crustal structure of the Jazmurian depression (Fig. 1), which is considered to be a fore-arc compressive basin, varies laterally. The eastern Jazmurian shows lower velocities in the upper crust than does the western Jazmurian. The low velocity (< 3.1 km/s) boundary is around 10 km in the eastern Jazmurian, but the western half shows shallower sedimentary thickness. Given the proximity of the Jazmurian depression to the Sistan suture further east, the thick sedimentary basin of the eastern Jazmurian might be a consequence of the closure of the Neotethys during Jurassic and Cretaceous times (Agard et al., 2011) as part of its accretionary complex.

Another large/deep low-speed anomaly in the upper crust is observed in the volcanic belt of the Makran Subduction

Zone (Fig. 6-e). Similar to the Lorestan low anomaly, the low V_s zone under the Taftan volcano and the southern Sistan belt is very deep (> 25 km). In this region, we expect to have the mantle wedge of the subduction, where the oceanic plate deepens beneath the Iranian Plateau and arc magmas are generated. The magma migrates into the overlying crust, lowering the seismic wave speeds.

Our velocity model shows some regions of thick sediments in central Iran, including, the Dasht-e Kavir, Tabas, and the southern Lut blocks (labels "K" and "TB" in Fig. 6-e). The sedimentary basins of central Iran are not as thick as the Mesopotamia-Zagros-Makran basins. The basins reach a maximum depth of ~10 km in the Dasht-e Kavir. A band of low velocity anomaly extending from the southern Lut Block to the Tabas microplate is seen. This basin is also detected in the potential field data analyses on Iran (Teknik and Ghods, 2017; Mousavi and Ebbing, 2018). Although, Teknik and Ghods (2017) estimated the deepest basins of central Iran to around 15 km, other studies do not propose more than 10 km for the sediment covers of this region (e.g., Morley et al., 2009; Mousavi and Ebbing, 2018).

The central-western Alborz Mountains are a higher velocity region compared to the eastern Alborz. The region covering the eastern end of the Alborz, Binalud, and western Kopeh Dagh, shows low velocities in the shallow upper crust (Fig. 6a-b), which can be attributed to sedimentary covers of about 7-10 km. Teknik and Ghods (2017) identified a number of basins along the western Alborz-eastern Binalud range, but did not show any basins in western Alborz.

The SCB possesses a very thick sedimentary cover (e.g., Mangino and Priestley, 1998). The low V_s anomaly (< 3.1 km/s) representing the SCB sediments exceeds 20 km in depth in the western half of the basin. The CRUST1.0 global model (Laske et al., 2013) indicates that the deepest part of the SCB is 20 km thick. Elsewhere in the interior of the Plateau, some smaller basins such as the northern part of the Sistan belt (label "S" in Fig. 6-e) and a basin in northwest SSZ (label "B" in Fig. 6-e) also show low velocities at shallow depths. The CRUST1.0 model does not show significantly thick sediments for the internal basins of Iran.

4 Conclusions

We have presented a quasi-3D shear wave velocity model of the upper crust in the Iranian Plateau derived from fundamental mode Rayleigh wave group velocity inversion. The model has the advantage of a large data set comprising both ambient noise and regional earthquake measurements. As a result, it reveals more structural details of the upper crust of the region compared to the previous studies. The main conclusions are as follows:

1) The short period content (5-25 s) of ambient noise cross-correlations and regional earthquakes constrain the upper crustal structure. The low velocity anomalies of the shallow upper crust represent regions of thick sediment across the Iranian Plateau. Mesopotamia, the SFB, the Zagros foreland, and the Makran accretionary wedge together form an extensive zone of thick sedimentary basins. The SCB is also mapped as a very deep sedimentary basin. The inland basins of central Iran such as the Lut Block, the Jazmurian depression and the Dasht-e Kavir are characterized by low velocities and are bounded to less than 10 km of thickness.

2) We observe three anomalously deep (> 20 km) low shear wave velocity (< 3.1 km/s) regions: a) In the SCB, low velocities extend to more than 22 km deep in the western part, revealing the deepest section of the basin. b) In the southern part of the Lorestan Arc, low velocities

persist to greater depths than in any other region of the Zagros. The seismically active upper-to-middle crust with a thick layer of sediments topping the crushed crystalline basement can result in low V_s for the crust of this region. c) Under the region of the Taftan volcano in the southeast, the source of the observed low V_s in the upper crust is heat and possibly partial melt is transported upward from the mantle wedge above the subducting slab.
3) The velocity model of this study does not show extensive regions of significant high velocities anywhere in the upper crust. In the 14-22 km depth range, most of the high-velocity regions are limited to small patches along the southwestern margin of central Iran from the NW corner of Iran to the south of the Lut Block. These regions correlate with some of the igneous and metamorphic provinces of central Iran.

Acknowledgments
We thank two anonymous reviewers and the associate editor for their comments and constructive criticism.

References

Agard, P., Omrani, J., Jolivet, L., Whitechurch, H., Vrielynck, B., Spakman, W., Monie´, P., Meyer, B., and Wortel, R., 2011, Zagros orogeny: a subduction-dominated process: Geological Magazine, **148**(5-6), 692–725.

Alavi, M., 2007, Structures of the Zagros fold-thrust belt in Iran: American Journal of Science, **307**(9), 1064–1095.

Bensen, G., Ritzwoller, M., Barmin, M., Levshin, A., Lin, F., Moschetti, M., Shapiro, N., and Yang, Y., 2007, Processing seismic ambient noise data to obtain reliable broadband surface wave dispersion measurements: Geophys. J. I., **169**(3), 1239–1260.

Debayle, E., and Sambridge, M., 2004, Inversion of massive surface wave data sets: Model construction and resolution assessment: J. Geophys. Rese., Solid Earth, **109**(B2), 1978–2012.

François, T., Agard, P., Bernet, M., Meyer, B., Chung, S. L., Zarrinkoub, M. H., et al., 2014, Cenozoic exhumation of the internal Zagros: First constraints from low-temperature thermochronology and implications for the build-up of the Iranian Plateau: Lithos, **206–207**(1), 100–112.

Gilligan, A., and Priestley, K., 2018, Lateral variations in the crustal structure of the Indo–Eurasian collision zone: Geophys. J. I., **214**(2), 975–989.

Haberland, C., Mokhtari, M., Babaei, H. A., Ryberg, T., Masoodi, M., Partabian, A., and Lauterjung, J., 2020, Anatomy of a crustal-scale accretionary complex: Insights from deep seismic sounding of the onshore western Makran subduction zone, Iran: Geology, **49**(1), 3–7.

Hatzfeld, D., and Molnar, P., 2010, Comparisons of the kinematics and deep structures of the Zagros and Himalaya and of the Iranian and Tibetan plateaus and geodynamic implications: Review of Geophysics, 48, RG2005, doi:10.1029/2009RG000304.

Herrmann, R. B., 2013, Computer programs in seismology: An evolving tool for instruction and research: Seismo. Res. Lett., **84**(6), 1081–1088.

Hessami, K., Pantosti, D., Tabassi, H., Shabanian, E., Abbassi, M. R., Feghhi, K., and Solaymani, S., 2003, Paleoearthquakes and slip rates of the North Tabriz Fault, NW Iran: preliminary results: Annals of Geophysics, **46**(5).

Jackson, J., Priestley, K., Allen, M., and Berberian, M., 2002, Active tectonics of the south Caspian basin: Geophys. J. I., **148**(2), 214–245.

Karasözen, E., Nissen, E., Bergman, E. A., and Ghods, A., 2019, Seismotectonics of the Zagros (Iran) from orogen-wide, calibrated earthquake relocations: J. Geophys. Res., Solid Earth,

124.

Kaviani, A., Paul, A., Moradi, A., Martin Mai, P., Pilia, S., Boschi, L., Rümpker, G., Lu, Y., Tang, Z., and Sandvol, E., 2020, Crustal and uppermost mantle shear wave velocity structure beneath the Middle East from surface wave tomography: Geophys. J. I., **221**(2), 1349–1365.

Kennett, B. L., Engdahl, E., and Buland, R., 1995, Constraints on seismic velocities in the Earth from traveltimes: Geophys. J. I., **122**(1), 108–124.

Khorrami, F., Vernant, P., Masson, F., Nilfouroushan, F., Mousavi, Z., Nankali, H., Saadat, S. A., Walpersdorf, A., Hosseini, S., Tavakoli, P., et al., 2019, An up-to-date crustal deformation map of Iran using integrated campaign-mode and permanent GPS velocities: Geophys. J. I., **217**(2), 832–843.

Kopp, C., Fruehn, J., Flueh, E. R., Reichert, C., Kukowski, N., Bialas, J., and Klaeschen, D., 2000, Structure of the Makran subduction zone from wide-angle and reflection seismic data: Tectonophysics, **329**(1–4), 171–191.

Laske, G., Masters, G., Ma, Z., and Pasyanos, M., 2013, Update on CRUST1.0 - A 1-degree global model of Earth's crust: Geophysical Research Abstracts, **15**, Abstract EGU2013-2658.

Maggi, A., and Priestley, K., 2005, Surface waveform tomography of the Turkish–Iranian plateau: Geophys. J. I., **160**(3), 1068–1080.

Maheri-Peyrov, M., Ghods, A., Donner, S., Akbarzadeh-Aghdam, M., Sobouti, F., Motaghi, K., Hassanzadeh, M., Mortezanejad, G., Talebian, M., and Chen, L., 2020, Upper crustal structure of NW Iran revealed by regional 3-D Pg velocity tomography: Geophysical Journal International, **222**(2), 1093–1108.

Mangino, S., and Priestley, K., 1998, The crustal structure of the southern Caspian region: Geophys. J. I., **133**, 630–648.

Montagner, J., 1986, Regional three-dimensional structures using long-period surface waves: Annals of Geophysics, **4**(B3), 283–294.

Morley, C. K., Kongwung, B., Julapour, A. A., Abdolghafourian, M., Hajian, M., Waples, D., et al., 2009, Structural development of a major late Cenozoic basin and transpressional belt in central Iran: The Central Basin in the Qom-Saveh area: Geosphere, **5**(4), 325–362.

Motaghi, K., Shabanian, E., and Nozad-Khalil, T., 2020, Deep structure of the western coast of the Makran subduction zone, SE Iran: Tectonophysics, **776**, 228314.

Mousavi, N., and Ebbing, J., 2018, Basement characterization and crustal structure beneath the Arabia–Eurasia collision (Iran): A combined gravity and magnetic study: Tectonophysics, **731–732**, 155-171.

Mouthereau, F., 2011, Timing of uplift in the Zagros belt/Iranian Plateau and accommodation of late Cenozoic Arabia–Eurasia convergence: Geological Magazine, **148**(5–6), 726–738.

Movaghari, R., Javan Doloei, G., Nowrozi, M., and Sadidkhouy, A., 2014, Velocity structure of south-east of Iran based on ambient noise analysis: Journal of the Earth and Space Physics, **40**(2), 17-30, doi: 10.22059/JESPHYS.2014.50627.

Movaghari, R., and Javan Doloei, G., 2020, 3-D crustal structure of the Iran plateau using phase velocity ambient noise tomography: Geophys. J. I., **220**(3), 1555–1568.

Movaghari, R., Javan Doloei, G., Yang, Y., Tatar, M., and Sadidkhouy, A., 2021, Crustal radial anisotropy of the Iran Plateau inferred from ambient noise tomography: J. Geophys. Res., Solid Earth, **126**,

doi.org/10.1029/2020JB020236.

Paul, A., Hatzfeld, D., Kaviani, A., Tatar, M., and Pequegnat, C., 2010, Seismic imaging of the lithospheric structure of the Zagros mountain belt (Iran): Geological Society, London, Special Publications, **330**(1), 5–18.

Paul, A., Kaviani, A., Hatzfeld, D., Vergne, J., and Mokhtari, M., 2006, Seismological evidence for crustal-scale thrusting in the Zagros mountain belt (Iran): Geophys. J. I., **166**(1), 227–237.

Penney, C., Tavakoli, F., Saadat, A., Nankali, H. R., Sedighi, M., Khorrami, F., Sobouti, F., Rafi, Z., Copley, A., Jackson, J., and Priestley, K., 2017, Megathrust and accretionary wedge properties and behaviour in the Makran subduction zone: Geophys. J. I., **209**(3), 1800–1830.

Priestley, K., Baker, C., and Jackson, J., 1994, Implications of earthquake focal mechanism data for the active tectonics of the South Caspian Basin and surrounding regions: Geophys. J. I., **118**(1), 111–141.

Priestley, K., McKenzie, D., Barron, J., Tatar, M., and Debayle, E., 2012, The Zagros core: Deformation of the continental lithospheric mantle: Geochemistry, Geophysics, Geosystems, **13**, Q11014.

Rahimi, H., Hamzehloo, H., Vaccari, F., and Panza, G. F., 2014, Shear-Wave velocity tomography of the lithosphere-asthenosphere system beneath the Iranian Plateau: Bull. Seism. Soc. Am., **104**(6), 2782-2798.

Shad Manaman, N., Shomali, H., and Koyi, H., 2011, New constraints on upper-mantle S-velocity structure and crustal thickness of the Iranian plateau using partitioned waveform inversion: Geophys. J. I.,**184**(1), 247–267.

Tatar, M., Hatzfeld, D., Martinod, J., Walpersdorf, A., Ghafori-Ashtiany, M., and Chery, J., 2002, The present-day deformation of the central Zagros from GPS measurements: Geophys. Res. Lett., **29**(19), 33-1-33-4.

Teknik, V., and Ghods, A., 2017, Depth of magnetic basement in Iran based on fractal spectral analysis of aeromagnetic data: Geophys. J. I., **209**, 1878–1891.

Vernant, P., Nilforoushan, F., Chery, J., Bayer, R., Djamour, Y., Masson, F., Nankali, H., Ritz, J.-F., Sedighi, M., and Tavakoli, F., 2004a, Deciphering oblique shortening of central Alborz in Iran using geodetic data: Earth and Planetary Science Letters, **223**(1-2), 177–185.

Vernant, P., Nilforoushan, F., Hatzfeld, D., Abbassi, M., Vigny, C., Masson, F., Nankali, H., Martinod, J., Ashtiani, A., Bayer, R., et al., 2004b, Present-day crustal deformation and plate kinematics in the Middle East constrained by GPS measurements in Iran and northern Oman: Geophys. J. I., **157**(1), 381–398.